J Radioanal Nucl Chem
DOI 10.1007/s10967-015-4360-6

Calibration of HPGe detectors using certified reference materials of natural origin

Gerti Xhixha[1] · Matteo Alberi[2] · Marica Baldoncini[2] · Kozeta Bode[3] · Elida Bylyku[3] · Florinda Cfarku[3] · Ivan Callegari[1] · Fadil Hasani[4] · Sheldon Landsberger[5] · Fabio Mantovani[2] · Eva Rodriguez[6] · Ferat Shala[7] · Virginia Strati[2] · Merita Xhixha Kaçeli[1]

Received: 13 April 2015

Abstract The feasibility of using certified reference materials for the full energy efficiency calibration of p-type coaxial high-purity germanium detectors for the determination of radioactivity in environmental samples is discussed. The main sources of uncertainty are studied and the contributions to the total uncertainty budget for the most intense gamma lines are presented. The correction factors due to self-absorption and true coincidence summing effects are discussed in detail. The calibration procedure is validated for natural and artificial radionuclide determination in different matrices through an internal cross-validation and through the participation in a world-wide open proficiency test.

✉ Gerti Xhixha
xhixha@fe.infn.it

[1] Legnaro National Laboratory, National Institute of Nuclear Physics, Via dell'Università 2, 35020 Legnaro, Padova, Italy

[2] Department of Physics and Earth Sciences, University of Ferrara, Via Saragat, 1, 44100 Ferrara, Italy

[3] Institute of Applied Nuclear Physics, Rr. Thoma Filipeu, Qesarakë, P.O. Box 85, Tiranë, Albania

[4] Kosovo Agency for Radiation Protection and Nuclear Safety (KARPNS), Office of the Prime Minister, Ish-Gërmia, 10000 Pristina, Kosovo

[5] Nuclear Engineering Teaching Lab, University of Texas, Pickle Research Campus R-9000, Austin, TX 78712, USA

[6] Centro de Investigaciones Energéticas, Medioambientales y Tecnológicas (CIEMAT), Avda de la Complutense 40, 28040 Madrid, Spain

[7] Faculty of Mechanical Engineering, University of Pristina "Hasan Prishtina", Bregu i Diellit, 10000 Pristina, Kosovo

Keywords Efficiency calibration · Certified reference material · HPGe gamma-ray spectrometry · Uncertainty budget · True coincidence summing · Self-absorption

Introduction

High-resolution gamma-ray spectrometry is a widely used non-destructive measurement technique for the assessment of gamma-ray emitting radionuclides present in environmental samples. The process of the determination of the full energy calibration is of great importance for the accurate determination of natural and anthropogenic radionuclides in environmental samples such as soils, sediments, rocks, foodstuffs and surface and ground water. In cases when standard gamma-ray emitting point or volume sources are not accessible, certified reference materials (CRMs) have been demonstrated to be a suitable calibration source for the determination of the detection efficiency of hyper-pure germanium (HPGe) detectors [1–3]. CRMs of natural origin are an effective solution due to both the relatively low cost and to the presence of radionuclides with very long half-lives with respect to standard sources. Another important advantage of CRMs is that they can be easily managed by individual laboratories in order to reproduce specific counting geometries and density ranges. Using CRMs is an appropriate solution for the determination of the environmental radioactivity as they contain radionuclides which cover an energy range from 46.5 keV (^{210}Pb) up to 2614 keV (^{208}Tl). When using CRMs, however, particular attention must be paid to the presence of interfering radionuclides which should be accurately investigated [4]. Moreover, the self-attenuation due to sample matrix and density can give non- negligible effects [1, 4, 5].

Published online: 14 August 2015

In this work, the CRMs RGK-1, RGU-1 and RGTh-1 traceable by the International Atomic Energy Agency (IAEA) [6] are used for the efficiency calibration of the MCA_Rad system entailing two p-type HPGe detectors [7, 8]. An analytical approach and a Monte Carlo simulation were used for the evaluation of the corrections due to self-absorption and true coincidence summing effects, respectively. A detailed study of the principal sources of uncertainty in order to assess the total uncertainty budget is performed. The description of the calibration process and the study of uncertainties presented in this work can be a useful guideline for a conscious use of CRMs for the determination of full energy efficiency of HPGe detectors.

The efficiency calibration was internally cross-validated by using phopshogypsum IAEA 434 [9] and oilfield contaminated soil IAEA 448 [10] CRMs. Finally, an external cross-validation was performed by participating to the world-wide open proficiency test organized by IAEA (TEL 2014-03).

Experimental

HPGe gamma-ray spectrometer set-up

The MCA_Rad system is made up two coaxial p-type HPGe detectors (certified by manufacturer with 60 and 67 % of relative efficiency respectively) with a measured energy resolution of approximately 1.9 keV at 1332.5 keV (^{60}Co). The HPGe detectors are coupled with a self-designed automatic sample changer, which allows managing independently the measurement of up to 24 samples without any human intervention. The system is well shielded principally with 10 cm of lead and 10 cm of copper, which reduces the laboratory background by approximately two orders of magnitude. The fully automated HPGe gamma-ray spectrometer, called MCA_Rad system has been previously is described in detail Xhixha et al. [7].

Measurement procedure

Gamma-ray spectrometry measurements are carried out simultaneously by the two HPGe detectors closely facing the opposite bases of a cylindrical polycarbonate sample container (7.5 cm in diameter and 4.5 cm in height). An a priori energy calibration procedure is performed by measuring the gamma radiation from a calibration source that covers the energy range from 186.2 keV (^{226}Ra) to 2614.5 keV (^{208}Tl). The energy and FWHM (Full Width at Half Maximum) determined for the most intense photopeaks are well fitted with a first order (Eq. 1) and a second order (Eq. 2) polynomial function, respectively, with a reduced $\chi^2 = 1.0$.

$$E(\text{keV}) = a_1 \times \text{Channel} + a_2 \quad (1)$$

$$\text{FWHM(keV)} = b_1 \times E^2 + b_2 \times E + b_3 \quad (2)$$

where the fitting coefficients for Eq. (1) are 0.40, 0.91 for HPGe A and 0.40, 1.05 for HPGe B, while for Eq. (2) are -6.11×10^{-8}, 7.25×10^{-4}, 9.76×10^{-1} for HPGe A and -6.83×10^{-8}, 8.34×10^{-4}, 8.81×10^{-1} for HPGe B (Fig. 1).

After energy calibration, the spectra were rebinned by extracting pseudorandom numbers according to a Gaussian probability density function. The reference energy calibration function has a zero offset and 0.35 keV per channel. The stability of the energy calibration is monitored periodically and the calibration is repeated if a shift larger than 0.5 keV is observed. A check on possible systematics introduced by the rebinning process was performed. Although the procedure was found to be dependent on the count rates, the amplitude of the fluctuations was always within the statistical counting uncertainty for this energy range and accordingly the net peak areas are not affected. Finally, the spectrum assigned to the single measurement is obtained by adding the two rebinned spectra.

Absolute efficiency determination and uncertainty analysis

Certified reference material preparation and measurement

The photopeak efficiency calibration was determined using three CRMs released by the IAEA and coded as RGU-1, RGTh-1 and RGK-1. The specific activities of the CRMs are certified at 95 % confidence level and are equal to 4940 ± 30 Bq/kg for ^{238}U (RGU-1), 3250 ± 90 Bq/kg for ^{232}Th (RGTh-1) (both in secular equilibrium) and to 14,000 ± 400 Bq/kg for ^{40}K (RGK-1) [6]. The CRMs, already prepared in powder matrix (240 mesh) are dried at a temperature of 60 °C until a constant weight is achieved and transferred into the standard counting geometry. Each standard sample is accurately sealed using vinyl tape and then left undisturbed for at least 4 weeks in order to establish radioactive equilibrium between ^{226}Ra and ^{222}Rn prior to be measured. In the case of materials characterized by high radon exhalation, the sealing is very important in order to reduce the ^{222}Rn loss [11, 12]. The sealing effectiveness and consequently the ^{222}Rn growth within the container were successfully checked, as shown in Fig. 2 where the in-grow of count rates of radon progeny ^{214}Bi (at 609 keV) is displayed for a phosphogypsum sample. The

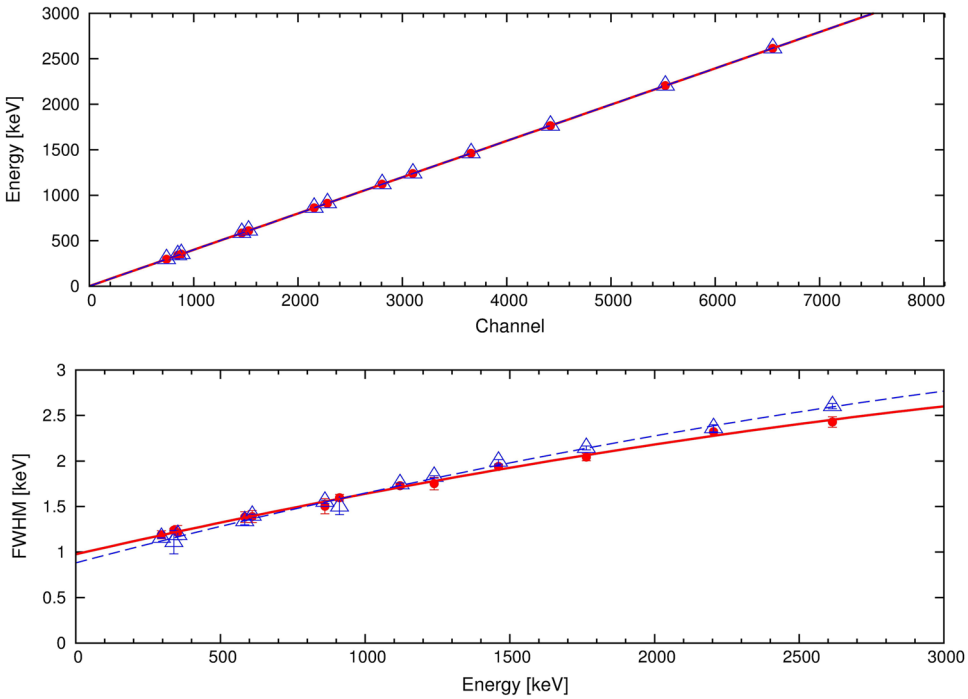

Fig. 1 The energy and FWHM calibration of both HPGe detectors constituting the MCA_Rad system: continuous *red line* and *red circles* are referred to HPGe A, *dashed blue line* and *blue triangles* are referred to HPGe B. (Color figure online)

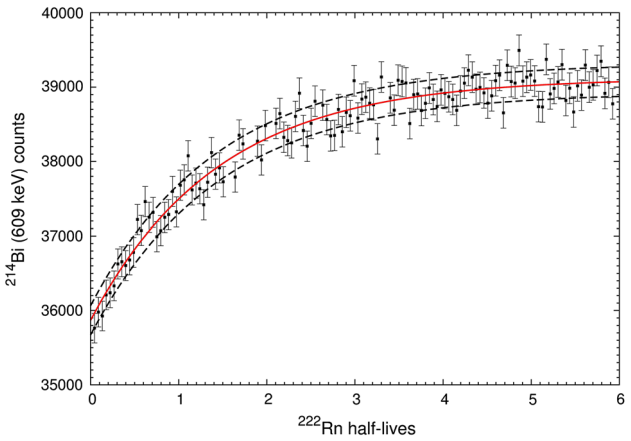

Fig. 2 The radon daughter ^{214}Bi (at 609 keV) counts growth measured in standard counting geometry for six ^{222}Rn half-lives. Each data point corresponds to 4-hour measurements. The continuous *red line* represents the fitting curve and *dashed black line* represents the one sigma uncertainty. (Color figure online)

in-growth counts were measured for six ^{222}Rn half-lives (corresponding to approximately 99 % of equilibrium). The experimental data points are well fitted (with a reduced $\chi^2 = 1.0$) taking the ^{222}Rn half-live (3.821 days [13] as a fixed parameter.

The reproducibility of source positioning and instrument stability was checked by sequentially measuring the CRM for 1 h acquisition time for 12 h, first without removing the CRM from one measurement to the following one and secondly by removing the CRM at the end of each measurement. In Tables 1 and 2 are shown the statistical uncertainties and the standard deviation ($\pm 1\sigma$) for the count rates of the most intense gamma emissions, which are used for determining the photopeak efficiency curve. The corrected net peak area (N) for the background was obtained according to the expression ($N = N_{\mathrm{CRM}} - \left(t_{\mathrm{L,CRM}}/t_{\mathrm{L,bckg}}\right)N_{\mathrm{bckg}}$), where N_{CRM}, N_{bckg} are the net peak areas in the CRM spectrum and background spectrum, respectively, and $t_{\mathrm{L,CRM}}$, $t_{\mathrm{L,bckg}}$ are the respective acquisition live times. The combined uncertainty is derived by applying the uncertainty propagation law for the no-correlation case, as the CRM spectrum comes from the sum of the two HPGe uncorrelated spectra, which in turn are not correlated to the background spectrum.

The standard deviation of the precision was found to be generally comparable with the counting uncertainty. In the case of measurements during repeated removing of the samples, the standard deviation of the precision slightly increased with respect to the previous case. As a result of these tests, the uncertainties due to the measurement repeatability (source positioning, homogeneity) and to instrument stability (background fluctuation) are found negligible with respect to the counting uncertainty.

Absolute efficiency calculation and uncertainty analysis

The photopeak efficiency ($\varepsilon_{\mathrm{CRM}}(E_i)$) can be expressed in general by the following formula:

Table 1 The precision with statistical uncertainty and 1σ standard deviation of twelve repeated measurements (1 h live time) in counts per second (cps) without removing the sample

	^{234m}Pa (1001 keV)	^{214}Pb (351 keV)	^{214}Bi (609 keV)	^{228}Ac (911 keV)	^{212}Pb (238 keV)	^{212}Bi (727 keV)	^{208}Tl (583 keV)	^{40}K (1460 keV)
Precision (stat. unc.) ± std. deviation	0.33 $(2)_{stat} \pm 0.02$	26.01 $(9)_{stat} \pm 0.07$	19.95 $(8)_{stat} \pm 0.08$	6.46 $(4)_{stat} \pm 0.08$	25.32 $(29)_{stat} \pm 0.09$	2.02 $(3)_{stat} \pm 0.03$	8.83 $(5)_{stat} \pm 0.05$	9.05 $(5)_{stat} \pm 0.04$
Rel. unc. (%)	6.06	0.27	0.40	1.24	0.35	1.48	0.57	0.44

$$\varepsilon_{CRM}(E_i) = \frac{N}{A_{CRM} t_{L,CRM} I_\gamma(E_i) m_{CRM}} \times \frac{1}{C_{SA}} \frac{1}{C_{TCS}} \frac{1}{C_{D_1}} \frac{1}{C_{D_2}} \frac{1}{C_{D_3}} \frac{1}{C_{RS}} \frac{1}{C_G} \quad (3)$$

where A_{CRM} is the certified activity concentration (in Bq/kg) of the CRMs, $I_\gamma(E_i)$ is the gamma-ray energy emission probability corrected for the branching ratio, m_{CRM} is the mass (in kg) of the CRMs, C_{D1}, C_{D2}, C_{D3} are respectively the decay correction factors for radionuclide decay during sampling period, during the end of sampling until the start of the measurement period and during the counting period, C_{RS} is the correction factor for random summing effect, C_G is the correction factor for different counting geometries, C_{SA} is the correction factor for mass density and atomic composition differences and C_{TCS} is the correction factor for the true coincidence summing effect. The decay data for natural radionuclides are taken from DDEP (Decay Data Evaluation Project)—LNHB Atomic and Nuclear Data [14–18].

Negligible corrections

The corrections for nuclide decay are negligible, since the half-lives of natural radionuclides are much longer compared to sampling (C_{D1}), storage (C_{D2}) and counting (C_{D3}) periods: e.g. for experimental time periods of <1 % of nuclide half-life the magnitude of the correction factor is <<1 % and therefore can be neglected. On the other hand, when all corrections are needed, attention must be paid to the correlation among the three correction factors [19].

The correction on the random summing is considered negligible since the dead time is too low for low count rates which are of the order of few hundreds of cps. However, corrections for random summing effect (C_{RS}) has to be taken into account for high dead time. Moreover, in cases when the standard geometry is identical to the counting geometry, as in our case, the correction due to geometrical differences becomes virtually negligible. In different situations the geometrical corrections must be determined. An experimental approach for correcting for the geometrical factor when using standard point sources for absolute efficiency calibration has been previously shown by Xhixha et al. [7].

Self-absorption correction

As the activity of the samples is determined based on the efficiency curve $\varepsilon(E)$ established for a calibration source, departures in sample chemical composition and density with respect to the standard have to be considered in order to account for different photon attenuation within the source material itself. In our approach the correction factor

Table 2 The precision with statistical uncertainty and 1σ standard deviation of twelve repeated measurements (1 h live time) in counts per second (cps) removing the sample at the end of each measurement

	^{234m}Pa (1001 keV)	^{214}Pb (351 keV)	^{214}Bi (609 keV)	^{228}Ac (911 keV)	^{212}Pb (238 keV)	^{212}Bi (727 keV)	^{208}Tl (583 keV)	^{40}K (1460 keV)
Precision (stat. unc.) ± std. deviation	0.33 $(2)_{stat}$ ± 0.02	26.07 $(9)_{stat}$ ± 0.14	19.96 $(8)_{stat}$ ± 0.10	6.44 $(4)_{stat}$ ± 0.03	25.30 $(27)_{stat}$ ± 0.10	2.02 $(3)_{stat}$ ± 0.04	8.80 $(5)_{stat}$ ± 0.06	9.08 $(5)_{stat}$ ± 0.05
Rel. unc. (%)	6.06	0.54	0.50	0.47	0.39	1.98	0.68	0.55

for the self-attenuation effect (C_{SA}) is determined considering that the mass attenuation coefficient is strongly dependent on the atomic composition below few hundred of keV, while for the energy range 200–3000 keV it can be well approximated with the average with a standard deviation of less than 2 % [7, 8, 20]. Differently from the analytical approach discussed by Xhixha et al. [7], the C_{SA} was estimated by performing a Monte Carlo simulation in which the counting geometry was modeled as entirely composed by one major oxide at time. The Z-effective of the investigated minerals (SiO_2, Al_2O_3, CaO, MgO, FeO, K_2O, Fe_2O_3, $CaCO_3$, Na_2O, P_2O_5, MnO) range between 9.99 and 17.16 at 1 MeV [21]. For each chemical composition are considered homogeneous materials having densities from 0.75 to 2.25 g/cm^3 typical of environmental samples. The simulation was performed for each sample counting condition by isotropically generating some 10^5 gammas having energy from 200 up to 3000 keV. The C_{SA} was estimated as the ratio between the number of emitted and transmitted photons accordingly to the standard counting geometry.

However, particular attention must be paid to the case of Naturally Occurring Radioactive Materials (NORMs) generated in industrial processes, which can lead to the concentration of chemical elements other than radioelements. A typical example is the case of scales from oil and gas exploration [22] in which an accumulation of calcium, strontium and barium is generally observed, severely affecting the attenuation of gamma rays. Another case of study which involves titanium oxide production industry [23] shows the importance of self-absorption correction, which can be studied with transmission method. In addition, the matrix composition can be determined using additional measurements by X-ray fluorescence spectrometry (XRF), neutron activation analysis (NAA) etc.

The C_{SA} exhibits a linear dependence on the sample density [24], where the intercept and the slope are functions of the photon energy, as stated in the following relationship:

$$C_{SA}(\rho, E) = A(E) + B(E)\rho. \quad (4)$$

The intercept was parametrized with respect to the photon energy (E) according to the following expression $A(E) = \sum_{i=0}^{3} a_i E^{-i}$ and the dependence of the slope on the photon energy (E) is equal to that of the mass attenuation coefficient, which is well approximated by a second order polynomial of the logarithm of the energy $B(E) = \sum_{i=0}^{2} b_i \ln(E)^i$. The C_{SA} surface shown in Fig. 3 was obtained by performing a two-dimensional fit according to Eq. (4) with a reduced $\chi^2 = 1.0$. The input data points correspond to the C_{SA} determined for each sample density and for each photon energy as the uncertainty-weighted average among

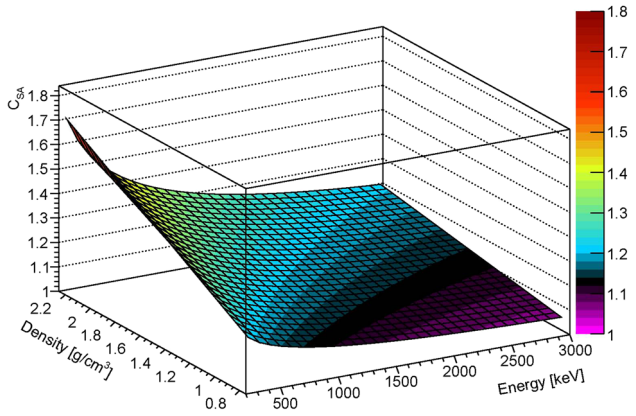

Fig. 3 The correction factor for self-absorption effect (inorganic material matrix) for the MCA_Rad counting geometry determined via Monte Carlo simulation as a function of sample density and photon energy. The Eq. (4) is fitted with the following parameters $a_0 = 1.00$, $a_1 = -5{,}96$, $a_2 = -2.99 \times 10^3$, $a_3 = 5.66 \times 10^5$ and $b_0 = 1.77$, $b_1 = -0.37$, $b_2 = 0.02$ with a reduced $\chi^2 = 1.0$

the values attained for the eleven different chemical compositions. The percentage uncertainties plotted in Fig. 4 correspond to the maximum variability with respect to the sample chemical composition of the C_{SA} (Fig. 3).

The same procedure was followed separately for organic material and water obtaining the correction factor for self-absorption as function of density and energy.

True coincidence summing correction

The correction factor for the true coincidence summing effect is determined using the mathematical formalism

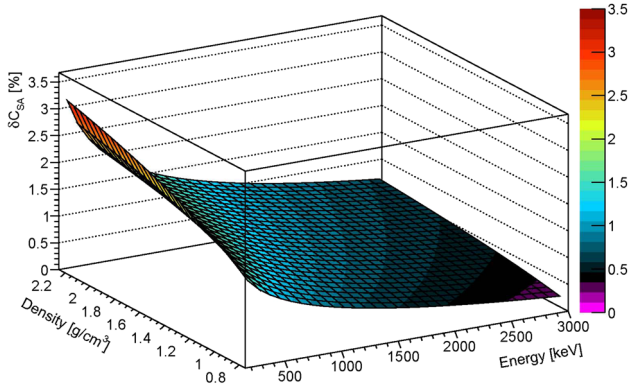

Fig. 4 The percentage uncertainty on the C_{SA} estimated in as the maximum variability of the correction factor with respect to the sample chemical composition

described by De Felice et al. [25] and in particular, the coincidence summing (both summing-in and summing-out effects) of $\gamma - \gamma$ can be modeled as:

$$C_{TCS}(i) = \left(1 - \frac{\sum_j P_{t(i,j)} P_{(i)} P_{(j)} \varepsilon_{t(j)}}{I_{\gamma(i)}}\right) \left(1 + \frac{\sum_{k,m} P_{t(k,m)} P_{(k)} P_{(m)} \varepsilon_{p(k)} \varepsilon_{p(m)}}{I_{\gamma(i)} \varepsilon_{p(i)}}\right) \quad (5)$$

where $P(i)$ is the probability of photon emission in the i transition, $P_t(i,j)$ is the probability of the coincident transition $i - j$, $\varepsilon_p(i)$ is the apparent full energy peak efficiency for the energy of the transition i, and $\varepsilon_t(j)$ is the total apparent efficiency for the energy of the transition j. Since the relative efficiencies of both HPGe detectors are checked to be similar, the true coincidence summing effect is reasonably treated as a unique correction factor and applied to the final spectrum. In Table 3 are reported the correction equations for the true coincidence summing for the most intense gamma-rays as function of the "apparent" full energy peak efficiency (ε_p) and total efficiency (ε_t) calculated using decay data from Bé et al. [14–18]. The contribution of terms (coincident energies) having coefficients of less than five per thousand is not considered since their contribution in the correction factor is generally on the order of fractions of a percent. The correction equations are found to be comparable with those calculated in other studies [26–28], within few percent on the coefficients terms.

The "apparent" full energy peak efficiency (ε_p) and total efficiency (ε_t) (Fig. 5) are determined as described in Xhixha et al. [7], by measuring peak-to-total ratio using Eq. (6). The peak-to-total ratio was determined by measuring the single gamma-ray emitting radionuclides ^{137}Cs (661.6 keV), ^{241}Am (59.4 keV) and close energy gamma-ray emitting radionuclides ^{60}Co (average energy 1252.5 keV), ^{57}Co (average energy 124 keV). In the case of ^{22}Na (511 keV corrected for 1274 keV) the peak-to-total ratio was instead interpolated from other energies as described in [29]. Different approaches on calculation of total efficiency are described in De Felice et al [25].

$$\varepsilon_t(E) = \frac{\varepsilon_p(E)}{(P/T)} \quad (6)$$

The uncertainty of less than 10 % in the total efficiency was found to contribute to the uncertainty in coincidence summing correction factors between 1 and 2 % using Gaussian propagation law. The uncertainty of the correction factor for true coincidence summing for nuclides with complex decay schemes is found to be relatively higher (order of 5 %) which has been confirmed also by Sima et al. [30] and De Felice et al [25].

Table 3 Expressions of coincidence-summing correction factors determined for the most intense gamma emissions of a selected set of nuclides

Parent nuclide	Daughter nuclide	E (keV)	Iγ (%)	C_{TCS}	C_{TCS}
^{238}U	^{214}Pb	351.9	35.60	$\{1 - 0.0092\ \varepsilon_{t(478.1)}\}$	0.9983 (2)
		295.2	18.41	$\{1 + 0.0284\ \varepsilon_{p(242.0)}\ \varepsilon_{p(53.2)}/\varepsilon_{p(295.2)}\}$	1.0007 (1)
		242.0	7.27	$\{1 - 0.0720\ \varepsilon_{t(53.2)}\}$	0.9980 (2)
	^{214}Bi	609.3	45.49	$\{1 - 0.3212\ \varepsilon_{t(1120.3)} - 0.1256\ \varepsilon_{t(1238.1)} - 0.1054\ \varepsilon_{t(768.4)} - 0.0668\ \varepsilon_{t(934.1)} - 0.0524\ \varepsilon_{t(1408.0)} - 0.0458\ \varepsilon_{t(1509.2)} - 0.0352\ \varepsilon_{t(1155.2)} - 0.0330\ \varepsilon_{t(665.4)} - 0.0309\ \varepsilon_{t(1281.0)} - 0.0287\ \varepsilon_{t(1401.5)} - 0.0272\ \varepsilon_{t(806.2)} - 0.0171\ \varepsilon_{t(1385.3)} - 0.0152\ \varepsilon_{t(1583.2)} - 0.0098\ \varepsilon_{t(1207.7)} - 0.0103\ \varepsilon_{t(703.1)} - 0.0085\ \varepsilon_{t(719.9)} - 0.0086\ \varepsilon_{t(1538.5)} - 0.0062\ \varepsilon_{t(454.8)} - 0.0074\ \varepsilon_{t(1838.4)} - 0.0070\ \varepsilon_{t(388.9)} - 0.0070\ \varepsilon_{t(1052.0)} - 0.0069\ \varepsilon_{t(1599.3)} - 0.0059\ \varepsilon_{t(1594.8)} - 0.0055\ \varepsilon_{t(1133.7)} - 0.0668\ \varepsilon_{t(934.1)} - 0.0126\ \varepsilon_{tXK(81.0)}\}$	0.844 (46)
		1764.5	15.31	$\{1 - 0.0206\ \varepsilon_{t(964.1)}\}\{1 + 0.1047\ \varepsilon_{p(609.3)}\ \varepsilon_{p(1155.2)}/\varepsilon_{p(1764.5)} + 0.0091\ \varepsilon_{p(1377.7)}\ \varepsilon_{p(386.8)}/\varepsilon_{p(1764.5)}\}$	1.003 (1)
		1120.3	14.91	$\{1 - 0.9800\ \varepsilon_{t(609.3)} - 0.0216\ \varepsilon_{t(388.9)} - 0.0069\ \varepsilon_{t(752.8)} - 0.0050\ \varepsilon_{t(474.5)} - 0.0191\ \varepsilon_{tXK(81.0)}\}\ \{1 + 0.0192\ \varepsilon_{p(454.8)}\ \varepsilon_{p(665.4)}/\varepsilon_{p(1120.3)}\}$	0.823 (17)
		1238.1	5.83	$\{1 - 0.9800\ \varepsilon_{t(609.3)}\}\ \{1 + 0.0057\ \varepsilon_{p(832.4)}\ \varepsilon_{p(405.7)}/\varepsilon_{p(1238.1)} + 0.0121\ \varepsilon_{p(572.8)}\ \varepsilon_{p(665.5)}/\varepsilon_{p(1238.1)} + 0.0125\ \varepsilon_{p(469.8)}\ \varepsilon_{p(768.4)}/\varepsilon_{p(1238.1)}\}$	0.832 (17)
		2204.2	4.91	$\{1 + 0.0136\ \varepsilon_{p(543.0)}\ \varepsilon_{p(1661.3)}/\varepsilon_{p(2204.2)} + 0.0116\ \varepsilon_{p(826.5)}\ \varepsilon_{p(1377.7)}/\varepsilon_{p(2204.2)} + 0.0547\ \varepsilon_{p(1594.8)}\ \varepsilon_{p(609.3)}/\varepsilon_{p(2204.2)}\}$	1.005 (1)
^{232}Th	^{208}Tl	2614.5	99.76	$\{1 - 0.8500\ \varepsilon_{t(583.2)} - 0.2250\ \varepsilon_{t(510.7)} - 0.1240\ \varepsilon_{t(860.5)} - 0.0660\ \varepsilon_{t(277.4)} - 0.0180\ \varepsilon_{t(763.5)} - 0.0075\ \varepsilon_{t(252.7)} - 0.0701\ \varepsilon_{tKX(76.6)}\}$	0.762 (16)
		583.2	85.00	$\{1 - 0.9975\ \varepsilon_{t(2614.5)} - 0.2594\ \varepsilon_{t(510.7)} - 0.0761\ \varepsilon_{t(227.4)} - 0.0208\ \varepsilon_{t(763.5)} - 0.0087\ \varepsilon_{t(252.7)} - 0.0578\ \varepsilon_{tKX(76.6)}\}$	0.803 (13)
		860.5	12.40	$\{1 - 0.9975\ \varepsilon_{t(2614.5)} - 0.0136\ \varepsilon_{t(233.4)}\}\ \{1 + 0.5216\ \varepsilon_{(277.4)}\ \varepsilon_{(583.2)}/\varepsilon_{t(860.5)}\}$	0.932 (16)
	^{228}Ac	911.2	26.20	$\{1 - 0.0065\ \varepsilon_{t(57.8)} - 0.0175\ \varepsilon_{t(154.0)} - 0.0069\ \varepsilon_{t(199.4)} - 0.1033\ \varepsilon_{t(463.0)} - 0.0207\ \varepsilon_{t(562.5)} - 0.0239\ \varepsilon_{t(755.3)}\}$	0.966 (2)
		338.3	11.40	$\{1 - 0.0327\ \varepsilon_{t(1247.0)} - 0.0069\ \varepsilon_{t(948.0)} - 0.0380\ \varepsilon_{t(830.5)} - 0.0948\ \varepsilon_{t(772.3)} - 0.0424\ \varepsilon_{t(726.9)} - 0.0052\ \varepsilon_{t(620.3)} - 0.0075\ \varepsilon_{t(583.4)} - 0.0140\ \varepsilon_{t(478.4)} - 0.0097\ \varepsilon_{t(572.3)} - 0.0065\ \varepsilon_{t(57.8)}\}\ \{1 + 0.0735\ \varepsilon_{p(209.3)}\ \varepsilon_{p(128.2)}/\varepsilon_{p(338.3)}\}$	0.955 (3)

Terms for γ-KX-ray coincidence summing are taken from bibliography [26–28]

Efficiency curve fitting

The absolute efficiency is determined for the energy range from 160 to 2650 keV by using the function described in Tsoulfanidis and Landsberger [31] and Knoll [32] (Fig. 6):

$$\varepsilon(E_i) = \left(\frac{a_0}{E/E_0}\right)^{a_1} + a_2 \exp\left(-a_3 \frac{E}{E_0}\right) + a_4 \exp\left(-a_5 \frac{E}{E_0}\right) \quad (7)$$

where a_i are the six fitting parameters (with fitting values equal to $a_0 = 0.04$, $a_1 = -0.54$, $a_2 = -1.26$, $a_3 = 0.14$, $a_4 = -1.26$ and $a_5 = 0.14$). This function fits the data with a reduced $\chi^2 = 0.9$ with residues with respect to the fitting curve of generally less than 5 %. The energy range of validity of the fitting curve is not critical for the efficiency calibration of the MCA_Rad system since p-type HPGe gamma-ray spectrometers are not suitable for measuring low energy gamma-ray emitting radionuclides in environmental samples.

Assessment of the total uncertainty budget

The combined standard uncertainty, $u_c(\varepsilon)$, of the full-energy peak efficiency (ε) was calculated from the relative standard uncertainties of its components x_i according to the JCGM [33] as:

$$u_c(\varepsilon) = \varepsilon \sqrt{\sum_{i=i}^{n} \left(\frac{\partial \varepsilon}{\partial x_i} \frac{u(x_i)}{x_i}\right)^2} \quad (8)$$

The uncertainty propagation law of Eq. (8) assumes that the x_i parameters are not correlated. A way to simplify the calculation of the partial derivatives in calculating the combined uncertainties is to use a spreadsheet approach presented by Kragten [34], which is based on a numerical calculation of the partial derivatives. The uncertainties of components are assessed either by Type A or by Type B evaluations. Type A evaluation is based on a statistical evaluation of measurement data, as in the case of the counting uncertainty which is normally evaluated

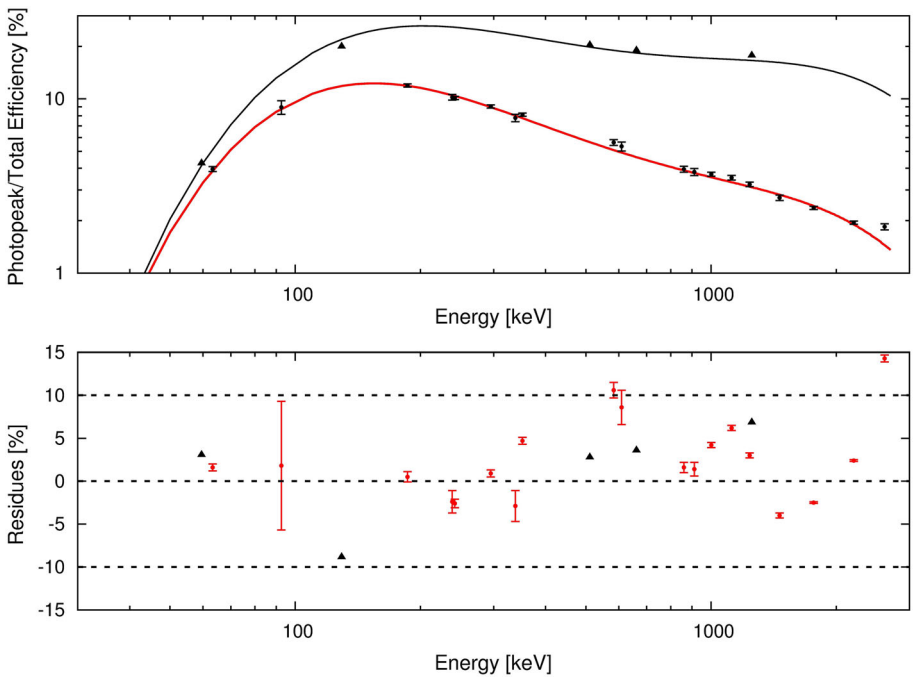

Fig. 5 Apparent photopeak efficiency and total efficiency determined for the MCA_RAD system. Residues show the percentage differences with respect to the fitting curve (logarithmic polynomial of the fifth order). *Black triangles* show the total efficiency determined experimentally as a cross-check

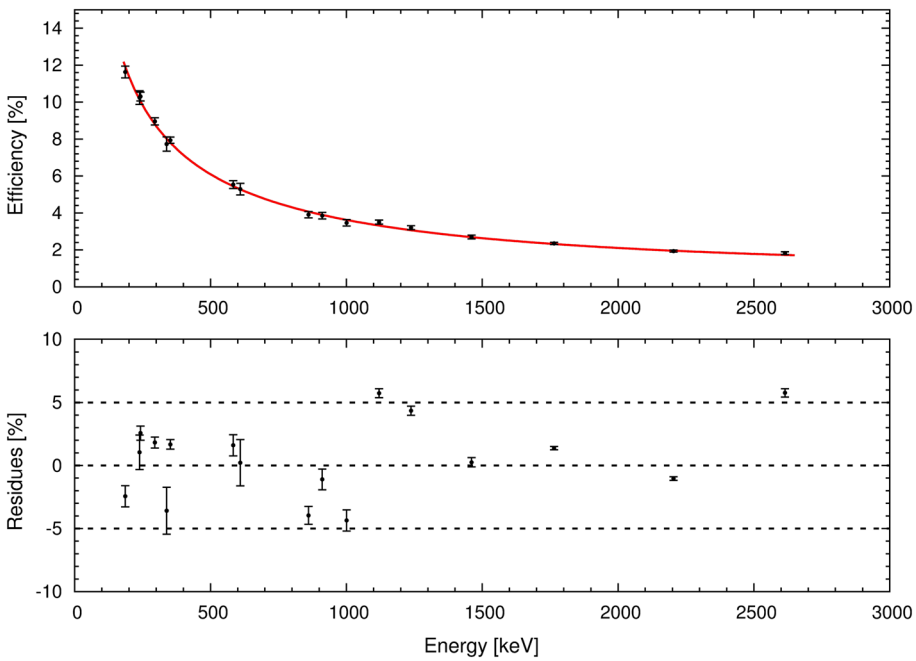

Fig. 6 Full energy peak efficiency determined for the MCA_Rad system. Residues show the percentage differences with respect to the fitting curve

according to the Poisson statistics. Type B evaluation is performed by any other method, e.g. in the case of data from certificates of reference materials or physical data from databases.

The relative contribution of the major components is given (Fig. 7) for the most intense gamma rays for all radionuclides present in the CRMs. The contribution to the combined uncertainty of the acquisition live time and of the sample mass is negligible for most gamma spectrometric applications. In the case of efficiency calibration, the counting statistics contribute to the combined uncertainty with few percent, except for the case of the low yield gamma-ray emitter ^{234m}Pa, where the counting statistics contribution is approximately 80 %. As it can be expected, the uncertainty on the CRM certified activity concentrations contribute to the uncertainty budget at the level of few percent for the RGU, while for the RGK and for the RGTh is the relative weight of this component is of

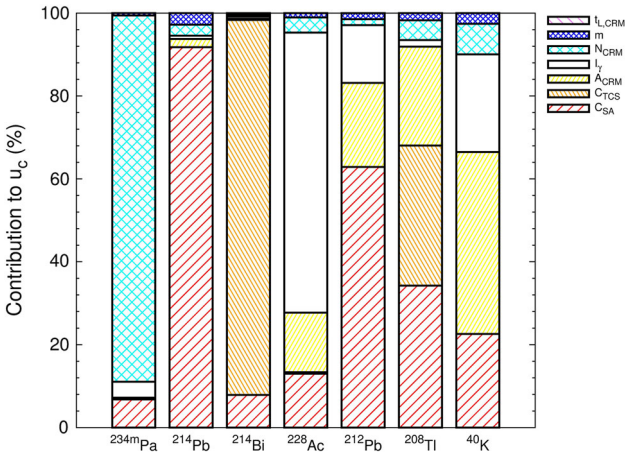

Fig. 7 The percentage relative contributions to the uncertainty budget of the major components entering in the efficiency calibration (Eq. 3) determination using CRMs

about 20 %. It is interesting to observe that a relatively high contribution to the combined uncertainty (about 60 %) comes from the gamma yield data of 911 keV (^{228}Ac). Indeed, this gamma line has approximately a 3 % relative uncertainty, which is relatively higher with respect to other gamma lines known with less than 1 % relative uncertainty. Finally, the major contribution to the combined uncertainty appears to come from the correction factor for the self-absorption effect, except for the 609 keV (^{214}Bi) gamma line, where the contribution of the correction factor due to the coincidence summing effect is dominant due to the ^{214}Bi complex decay scheme.

Experimental validation

The IAEA 434 [9] and IAEA 448 [10] certified reference materials were used to internally validate the efficiency calibration. The results (Table 4) show relatively good agreement within the uncertainty determined for the efficiency calibration. The disequilibrium in the decay chains of uranium and thorium [35] is taken into account for the IAEA 448 material by using the standard Bateman equation and by applying the appropriate decay correction factors to the results.

Moreover, an external validation was performed by participating in a world-wide proficiency test organized by IAEA (TEL 2014-03) on measuring environmental samples with different matrixes (water, hay, soil) which was organized by the IAEA. In Table 5 are reported the individual results for different matrices, evaluated by the IAEA in terms both of accuracy and of relative precision with respect to the target values.

Only in the case of ^{226}Ra in the water sample the relative bias was higher than the maximum acceptable value, although the internal quality control performed on sample 03-Water supplied by the IAEA (not shown) had satisfactory results. The relative bias was found to be −2.23 % (^{226}Ra), −2.04 % (^{137}Cs) and 0.76 % (^{134}Cs). The higher relative difference for ^{226}Ra in "02-Water" sample can be possibly attributed to accidental loss of radon.

Conclusions

In this work, is described the procedure for the efficiency calibration of p-type HPGe detectors using certified reference materials (CRMs). The hierarchy of the main sources of uncertainties including the self-absorption and true coincidence summing corrections is discussed in detail. A calibration of HPGe detectors using certified reference materials has been performed for the determination of natural and artificial radioactivity in environmental samples of different matrices. An exhaustive and reproducible experimental method based on an analytical approach and Monte Carlo simulation for estimating individual sources of uncertainty in HPGe efficiency calibration was completed. The full energy efficiency calibration of the MCA_Rad system was performed at less than 5 % accuracy for the energy range 200–2650 keV by using CRMs

Table 4 Cross-check control performed by measuring IAEA certified reference materials

Reference material	Matrix	Radionuclide	Certified activity (Bq/kg)	Measured activity (Bq/kg)	Relative bias (%)	Within 1σ agreement
IAEA-434	Phosphogypsum	^{226}Ra[a]	780 ± 62	747 ± 45	−4.23	Yes
IAEA-448	Soil from oil field	^{226}Ra[a]	19,050 ± 260	18,376 ± 1060	−3.54	Yes
		^{208}Tl[b]	555 ± 26	521 ± 32	−6.13	Yes
		^{212}Pb[b]	1623 ± 69	1578 ± 97	−2.77	Yes
		^{228}Ac[b]	1166 ± 55	1020 ± 65	−12.52	No
		^{40}K[b]	234 ± 12	244 ± 32	4.27	Yes

[a] Certified value

[b] Informative values

Table 5 Results from the IAEA evaluation in the framework of the world-wide open proficiency test IAEA-TEL-2014-03

Sample code	Radionuclide	IAEA target value ± combined uncertainty (Bq/kg, dry weight)	Laboratory value ± combined uncertainty (Bq/kg, dry weight)	Relative bias (%)	Final score
01-Water	^{134}Cs	21.4 ± 0.2	21.6 ± 1.3	0.93	A
	^{137}Cs	12.06 ± 0.1	11.6 ± 0.6	−3.81	A
02-Water	^{152}Eu	50.05 ± 0.41	53.0 ± 3.3	5.89	A
	^{226}Ra	**14.21 ± 0.06**	**10.5 ± 0.8**	**−26.11**	**N**
04-Seaweed	^{134}Cs	8.27 ± 0.2	8.0 ± 0.5	−3.26	A
	^{137}Cs	22.96 ± 0.45	21.4 ± 1.2	−6.79	A
	^{40}K	1780 ± 150	1672 ± 91.9	−6.07	A
05-Sediment	^{137}Cs	12 ± 0.4	12.2 ± 0.7	1.67	A
	^{228}Ac	12.1 ± 1.5	11.1 ± 0.9	−8.26	A
	^{40}K	270 ± 27	269.2 ± 14.9	−0.30	A
	^{212}Pb	12.2 ± 1.5	12.2 ± 0.7	0.00	A
	^{226}Ra	19 ± 4.8	17.8 ± 1.4	−6.32	A
	^{208}Tl	4.1 ± 0.7	4.8 ± 0.4	17.07	A

A stands for Accepted, *N* stands for Not Accepted

traceable by IAEA. The self-absorption effect is evaluated by Monte Carlo method as the ratio between emitted and transmitted gammas as a function of energy (200–2650 keV) and sample density (0.75–2.25 g/cm^3) for homogeneous samples composed by the main minerals present in rock and soil. The $\gamma - \gamma$ true coincidence summing was analytically determined as a relationship among gamma emission probabilities and total and absolute photopeak efficiencies. The hierarchy of uncertainties that commonly affect an HPGe gamma ray spectrometry measurement were evaluated. The relative contributions to 1σ combined uncertainty for the most intense gamma emission of each radionuclide present in the CRMs were determined. The non-negligible uncertainty due to self-absorption correction become relevant (more than 70 %) in particular for lower energy gamma lines of ^{214}Pb (351 keV) and ^{212}Pb (238 keV). The correction for true coincidence summing is negligible for all radionuclides, except in the case of ^{214}Bi and ^{208}Tl for which it is the most relevant contribution to the combined uncertainty. All radionuclides present in CRMs are suitable sources for accurate HPGe efficiency calibration, except for ^{234m}Pa that is not convenient due to its very low gamma yield. Finally, it is recommend a thoughtful choice of the nuclide datasheets because the gamma line intensity can be a dominant source of uncertainty as in the case of ^{228}Ac for the adopted DDEP (Decay Data Evaluation Project)—LNHB Atomic and Nuclear Data. The method was validated by measuring natural and artificial radionuclides in environmental samples of different matrices in the framework of an IAEA world-wide open proficiency test (IAEA-TEL-2014-03). An additional internal validation using certified reference material made up of NORM showed a 1σ level agreement, confirming the reliability of the efficiency calibration described.

Acknowledgements This work is supported by the MIUR (ITALRAD Project), by the Istituto Nazionale di Fisica Nucleare (INFN), by the Fondazione Cassa di Risparmio di Padova e Rovigo, and by NORM4BUILDING COST TU1301 project. The authors are grateful to William F McDonough, Roberta Rudnick, Catalina Gasco, Giovanni Fiorentini, Tommaso Colonna, Luigi Carmignani Carlos Rossi Alvarez, Giampietro Bezzon, Giampaolo Buso, Alessandro Zanon, Liliana Mou, Roberto Paulon and Mattia Taroni for the valuable discussion on the manuscript. The authors are grateful to the members of the mechanical laboratory of University of Ferrara for the technical support.

References

1. Ebaid YY (2009) On the use of reference materials in gamma-ray spectrometric efficiency calibration for environmental samples. J Radioanal Nucl Chem 280(1):21–25. doi:10.1007/s10967-008-7377-2
2. Nir-El Y (1998) Application of reference materials in the accurate calibration of the detection efficiency of a low-level gamma-ray spectrometry assembly for environmental samples. J Radioanal Nucl Chem 227(1–2):67–74. doi:10.1007/BF02386433
3. Iurian A-R, Cosma C (2014) A practical experimental approach for the determination of gamma-emitting radionuclides in environmental samples. Nucl Instrum Meth A 763:132–136. doi:10.1016/j.nima.2014.06.032
4. Oddone M, Giordani L, Giacobbo F, Mariani M, Morandi S (2008) Practical considerations regarding high resolution gamma-spectrometry measurements of naturally occurring radioactive samples. J Radioanal Nucl Chem 277(3):579–585. doi:10.1007/s10967-007-7113-3
5. Miller M, Voutchkov M (2014) The impact of uncertainty in the elemental composition of the certified reference material on

gamma spectrometry. J Radioanal Nucl Chem 299:551–558. doi:10.1007/s10967-013-2781-7
6. International Atomic Energy Agency (IAEA) (1987) Preparation and certification of IAEA gamma spectrometry reference materials, RGU-1, RGTh-1 and RGK1. Report-IAEA/RL/148. International Atomic Energy Agency, Vienna
7. Xhixha G, Bezzon GP, Broggini C, Buso GP, Caciolli A, Callegari I, De Bianchi S, Fiorentini G, Guastaldi E, Mantovani F, Massa G, Menegazzo R, Mou L, Pasquini A, Rossi Alvarez C, Shyti M, Kaçeli Xhixha M (2013) The worldwide NORM production and a fully automated gamma-ray spectrometer for their characterization. J Radioanal Nucl Chem 295:445–457. doi:10.1007/s10967-012-1791-1
8. Xhixha G, Ahmeti A, Bezzon GP, Bitri M, Broggini C, Buso GP, Caciolli A, Callegari I, Cfarku F, Colonna T, Fiorentini G, Guastaldi E, Mantovani F, Massa G, Menegazzo R, Mou L, Prifti D, Rossi Alvarez C, Sadiraj Kuqi Dh, Shyti M, Tushe L, Xhixha Kaçeli M, Zyfi A (2013) First characterization of natural radioactivity in building materials manufactured in Albania. Radiat Prot Dosim 155(2):217–223. doi:10.1093/rpd/ncs334
9. International Atomic Energy Agency (IAEA) (2010) Reference material IAEA 434: naturally occurring radionuclides in phosphogypusm. IAEA Analytical Quality in Nuclear Applications No. IAEA/AQ/17. International Atomic Energy Agency, Vienna
10. International Atomic Energy Agency (IAEA) (2013) Certified reference material IAEA-448: soil from oil field contaminated with technically enhanced radium-226. IAEA Analytical Quality in Nuclear Applications No. IAEA/AQ/30. International Atomic Energy Agency, Vienna
11. Scholten JC, Osvath I, Pham MK (2013) ^{226}Ra measurements through gamma spectrometric counting of radon progenies: how significant is the loss of radon? Mar Chem 156:146–152. doi:10.1016/j.marchem.2013.03.001
12. Mauring A, Gäfvert T (2013) Radon tightness of different sample sealing methods for gamma spectrometric measurements of ^{226}Ra. Appl Radiat Isot 81:92–95. doi:10.1016/j.apradiso.2013.03.022
13. Bellotti E, Broggini C, Di Carlo G, Laubenstein M, Menegazzo R (2915) Precise measurement of the ^{222}Rn half-life: a probe to monitor the stability of radioactivity. arXiv:1501.07757 [nucl-ex]
14. Bé M-M, Chisté V, Dulieu C, Browne E, Chechev V, Kuzmenko N, Helmer R, Nicholas A, Schönfeld E, Dersch R (2004) Monographie BIPM-5, table of radionuclides, vol 2. Bureau International des Poids et Mesures (BIPM), Sèvres
15. Bé M-M, Chisté V, Dulieu C, Browne E, Chechev V, Kuzmenko N, Kondev F, Luca A, Galán M, Pearce A, Huang X (2008) Monographie BIPM-5, table of radionuclides, vol 4. Bureau International des Poids et Mesures (BIPM), Sèvres
16. Bé M-M, Chisté V, Dulieu C, Mougeot X, Browne E, Chechev V, Kuzmenko N, Kondev F, Luca A, Galán M, Nichols AL, Arinc A, Huang X (2010) Monographie BIPM-5, table of radionuclides, vol 5. Bureau International des Poids et Mesures (BIPM), Sèvres
17. Bé M-M, Chisté V, Dulieu C, Mougeot X, Chechev VP, Kuzmenko NK, Kondev FG, Luca A, Galán M, Nichols AL, Arinc A, Pearce A, Huang X, Wang B (2011) Monographie BIPM-5, table of radionuclides, vol 6. Bureau International des Poids et Mesures (BIPM), Sèvres
18. Bé M-M, Chisté V, Dulieu C, Mougeot X, Chechev VP, Kondev FG, Nichols AL, Huang X, Wang B (2013) Monographie BIPM-5, table of radionuclides, vol 7. Bureau International des Poids et Mesures (BIPM), Sèvres
19. Makarewicz M (2005) Estimation of the uncertainty components associated with the measurement of radionuclides in air filters using g-ray spectrometry. Accred Qual Assur 10:269–276. doi:10.1007/s00769-005-0931-5
20. Kaminski S, Jakobi A, Wilhelm Chr (2014) Uncertainty of gamma-ray spectrometry measurement of environmental samples due to uncertainties in matrix composition, density and sample geometry. Appl Radiat Isot 94:306–313. doi:10.1016/j.apradiso.2014.08.008
21. Taylor ML, Smith RL, Dossing F, Franich RD (2012) Robust calculation of effective atomic numbers: the Auto-Zeff software. Med Phys 39:1769–1778
22. Landsberger S, Brabec C, Canion B, Hashem J, Lu C, Millsap D, George G (2013) Determination of ^{226}Ra, ^{228}Ra and ^{210}Pb in NORM products from oil and gas exploration: problems in activity underestimation due to the presence of metals and self-absorption of photons. J Environ Radioactiv 125:23–26. doi:10.1016/j.jenvrad.2013.02.012
23. Mantero J, Gázquez MJ, Hurtado S, Bolívar JP, García-Tenorio R (2015) Application of gamma-ray spectrometry in a NORM industry for its radiometrical characterization. Radiat Phys Chem. doi:10.1016/j.radphyschem.2015.02.018
24. Boshkova T, Minev L (2001) Corrections for self-attenuation in gamma-ray spectrometry of bulk samples. Appl Radiat Isot 54:777–783. doi:10.1016/S0969-8043(00)00319-5
25. De Felice P, Angelini P, Fazio A, Biagini R (2000) Fast procedures for coincidence-summing correction in γ-ray spectrometry. Appl Radiat Isot 52:745–752. doi:10.1016/S0969-8043(99)00239-0
26. Tomarchio E, Rizzo S (2011) Coincidence-summing correction equations in gamma-ray spectrometry with p-type HPGe detectors. Radiat Phys Chem 80:318–323. doi:10.1016/j.radphyschem.2010.09.014
27. Dryák P, Kovář P (2009) Table for true summation effect in gamma-ray spectrometry. J Radioanal Nucl Chem 279(2):385–394. doi:10.1007/s10967-007-7208-x
28. Schima FJ, Hoppes DD (1983) Tables for cascade-summing corrections in gamma-ray spectrometry. Appl Radiat Isot 34(8):1109–1114. doi:10.1016/0020-708X(83)90177-1
29. Debertin K, Helmer RG (1988) Gamma- and X-ray spectrometry with semiconductor detectors. North-Holland, Amsterdam, p 399. ISBN-13: 978-0444871077, ISBN-10: 0444871071
30. Sima O, Arnold D, Dovlete C (2001) GESPECOR: a versatile tool in gamma-ray spectrometry. J Radioanal Nucl Chem 248(2):359–364. doi:10.1023/A:1010619806898
31. Tsoulfanidis N, Landsberger S (2015) Measurement and detection of radiation, 4th edn. CRC Press, Taylor & Francis Group, Boca Raton, p 606. ISBN: 9781482215496
32. Knoll GF (2010) Radiation detection and measurement, 4th edn. Wiley, USA, p 860. ISBN: 978-0-470-13148-0
33. Joint Committee for Guides in Metrology (JCGM) (2008) Evaluation of measurement data Guide to the Expression of uncertainty in measurement JCGM 100:2008 (GUM 1995 with minor corrections). ISO/IEC Guide 98-3
34. Kragten J (1994) Calculating standard deviations and confidence intervals with a universally applicable spreadsheet technique. Analyst 119:2161–2165. doi:10.1039/AN9941902161
35. Michalik B, Brown J, Krajewski P (2013) The fate and behaviour of enhanced natural radioactivity with respect to environmental protection. Environ Impact Assess Rev 38:163–171. doi:10.1016/j.eiar.2012.09.001